

Silica-Supported Pentamethylcyclopentadienyl Ytterbium(II) and Samarium(II) Sites: Ultrahigh Molecular Weight Polyethylene without Co-Catalyst

Journal Article

Author(s):

Allouche, Florian; [Chan, Ka Wing](#) ; [Fedorov, Alexey](#) ; Andersen, Richard A.; [Copéret, Christophe](#) 

Publication date:

2018-03-19

Permanent link:

<https://doi.org/10.3929/ethz-b-000356698>

Rights / license:

[In Copyright - Non-Commercial Use Permitted](#)

Originally published in:

Angewandte Chemie 130(13), <https://doi.org/10.1002/ange.201800542>

Funding acknowledgement:

157146 - Monitoring active sites of metathesis catalysts: a combined operando spectroscopy and computational approach (SNF)

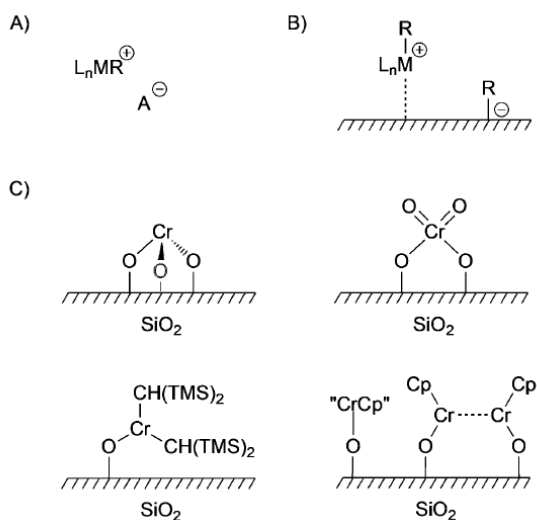
Silica-Supported Pentamethylcyclopentadienyl Ytterbium(II) and Samarium(II) Sites: Ultrahigh Molecular Weight Polyethylene without Co-Catalyst

Florian Allouche, Ka Wing Chan, Alexey Fedorov, Richard A. Andersen,* and Christophe Copéret*

Abstract: Designing highly active supported ethylene polymerization catalysts that do not require a co-catalyst to generate electrophilic metal alkyl species is still a challenge despite its industrial relevance. Described herein is the synthesis and characterization of well-defined silica-supported cyclopentadienyl Ln^{II} sites ($\text{Ln}=\text{Yb}$ and Sm) of general formula $[(\equiv\text{SiO})\text{LnCp}^*]$. These well-defined surface species are highly active towards ethylene polymerization in the absence of added co-catalyst. Initiation is proposed to occur by single electron transfer.

Polyethylene is one of the largest commodity chemicals, produced by the polymerization of ethylene using both homogeneous and heterogeneous catalysts. The formation of C–C bonds during ethylene polymerization takes place through the Cossee–Arlman mechanism which involves coordination of the incoming ethylene monomer to the open coordination site of an electrophilic metal alkyl species followed by an insertion step; the repetition of these two steps leads to polymer chain growth.¹ Generation of the catalytically active species, that is, an electrophilic metal alkyl species featuring an open coordination site, usually requires the use of a co-catalyst, for example, Ziegler–Natta catalysts or metallocenes (Scheme 1). The co-catalysts can be divided into two main categories, Lewis acids² such as $\text{B}(\text{C}_6\text{F}_5)_3$, or activators that function as alkylating agents and Lewis acids such as MAO or Et_3Al .^{2b, 2c, 3} In supported catalysts, the cationic metal alkyl can also be generated directly by reacting metal alkyl complexes using supports such as alumina⁴ and the Brønsted acidic sulfated oxides⁵ or alternatively by using supported MAO for

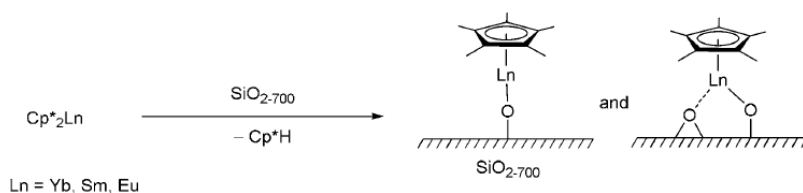
example.⁶ There are only a few heterogeneous catalysts that do not require such co-catalysts; the most prominent ones are the Phillips catalyst based on $\text{CrO}_3/\text{SiO}_2$,⁷ the related well-defined Cr^{III} silicates,⁸ the silica-supported $\text{Cr}[\text{CH}(\text{TMS})_2]_3$,⁹ and the Union Carbide system, $\text{Cp}_2\text{Cr}/\text{SiO}_2$.¹⁰ A similar parallel can be made for homogeneous systems. Probably the most noteworthy examples are based on Cp^*_2Ln ($\text{Ln}=\text{Yb}$ and Sm), that polymerize ethylene at room temperature.¹¹ The latter observations suggest that supporting these metallocenes, using the techniques of surface organometallic chemistry (SOMC),¹² can yield well-defined olefin polymerization catalysts working in absence of any co-catalysts. Here, we report the synthesis and the characterization of well-defined silica-supported cyclopentadienyl Ln^{II} sites, $[(\equiv\text{SiO})\text{LnCp}^*]$ with $\text{Ln}=\text{Sm}$ and Yb . These species efficiently polymerize ethylene in the absence of co-catalysts, and the initiation process most likely occurs through a single electron transfer.



Scheme 1. Proposed active sites in A) homogeneous and B) heterogeneous polymerization catalysts based on metal-alkyl cationic species. C) Rare examples of neutral initiating species active towards ethylene polymerization in the absence of a co-catalyst.

The reaction of an orange toluene solution of Cp^*_2Yb with silica, partially dehydroxylated at $700\text{ }^\circ\text{C}$ (SiO_{2-700} , $0.26\text{ mmol SiOH g}^{-1}$), yields a green material referred to as $\text{Cp}^*_2\text{Yb@SiO}_{2-700}$, (this notation refers to the formulation of the material prior to characterization) along with 0.79 equiv of Cp^*H with respect to the initial amount of silanol (Scheme 2). Elemental analysis (EA) of $\text{Cp}^*_2\text{Yb@SiO}_{2-700}$ gives

3.53 wt % Yb and 2.60 wt % C, corresponding to 10.6 C/Yb (10 expected); the amount of grafted complex is consistent with the release of 0.95 equiv of Cp*H per Yb center and the formation of surface monografted $[(\equiv\text{SiO})\text{YbCp}^*]$ species. Similarly, the green material $\text{Cp}^*_2\text{Sm@SiO}_{2-700}$ is obtained, along with 0.93 equiv of Cp*H per grafted Sm metallocene (EA: 2.82 wt % Sm and 2.16 wt % C, 9.6 C/Sm –10 expected).

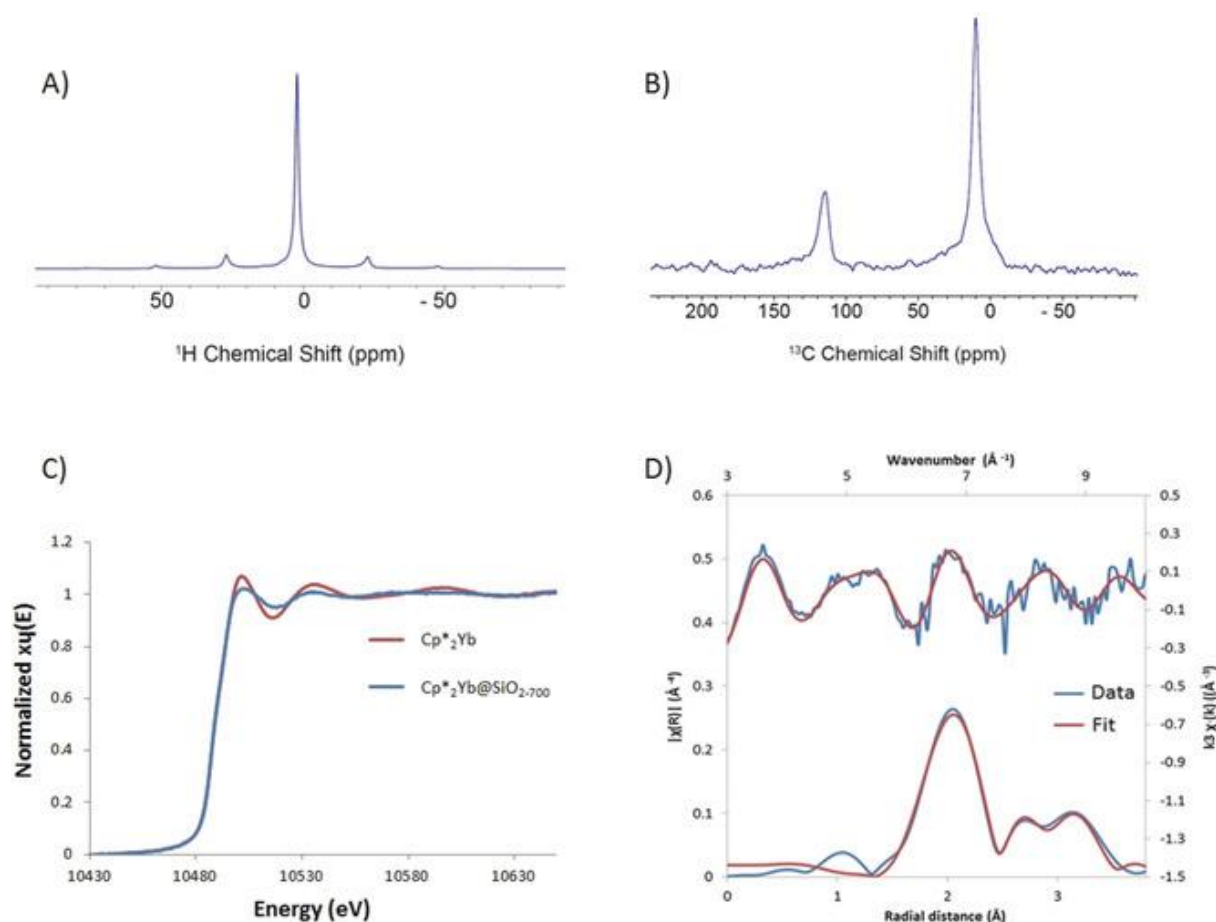


Scheme 2. Synthesis of $\text{Cp}^*_2\text{Ln@SiO}_{2-700}$.

Further characterization of $\text{Cp}^*_2\text{Ln@SiO}_{2-700}$ (Ln=Yb, Sm) by Fourier Transform infrared spectroscopy (FTIR—Figure S1 A) shows the presence of unreacted silanols as evidenced by the absorption at 3747 cm^{-1} and the appearance of a broad band centered at 3650 cm^{-1} , associated with silanols interacting with the grafted Ln organometallic fragments. The FTIR spectra are consistent with partial grafting; fewer Sm centers are grafted as evidenced by the presence of a larger amount of remaining isolated silanol groups, consistent with the lower Sm coverage obtained from elemental analysis (Figure S1A and the Supporting Information). Furthermore, contacting $\text{Cp}^*_2\text{Ln@SiO}_{2-700}$ with excess CO results in the appearance of a single IR band at 2161 cm^{-1} (Ln=Yb, Figure S1 B) and at 2167 cm^{-1} (Ln=Sm, Figure S1 C), which increases in intensity upon increasing the pressure of CO and disappears upon evacuation. The $\nu(\text{C}-\text{O})$ band is blue-shifted compared to free CO for both Ln=Yb and Sm. A similar trend, although less pronounced, is observed in the case of Cp^*_2Sm in solution with a $\nu(\text{C}-\text{O})$ band being blue-shifted to 2153 cm^{-1} .¹³ Nevertheless, the case of $\text{Cp}^*_2\text{Yb@SiO}_{2-700}$ is in contrast to the CO adducts of Cp^*_2Yb in solution in which the $\nu(\text{C}-\text{O})$ bands are red-shifted to 2114 and 2072 cm^{-1} , attributed to the presence of oxygen-

bonded CO according to DFT calculations.¹⁴ In $\text{Cp}^*_2\text{Yb}@SiO_{2-700}$, the CO is likely carbon-bonded in which the bonding of Yb–CO is mainly electrostatic, hence the blue shifted value.

In addition, the ^1H Magic angle spinning (MAS) NMR spectrum of $\text{Cp}^*_2\text{Yb}@SiO_{2-700}$ displays a single resonance with a chemical shift $\delta=0.76$ (Figure 1 A), and the ^{13}C cross-polarization magic angle spinning (CPMAS) NMR spectrum shows two resonances for the carbon atoms of the methyl and of the ring, respectively, at 10.1 and 114.5 ppm (Figure 1 B), slightly shifted with respect to Cp^*_2Yb observed at 10.6 and 113.4 ppm in solution. These data further support the formation of $[(\equiv\text{SiO})\text{YbCp}^*]$ as a well-defined silica-supported species.



A) 10 kHz magic angle spinning ^1H NMR spectrum of $\text{Cp}^*_2\text{Yb}@SiO_{2-700}$ B) 10 kHz cross-polarization magic angle spinning ^{13}C NMR spectrum of $\text{Cp}^*_2\text{Yb}@SiO_{2-700}$. C) Yb L_1 -edge XANES of Cp^*_2Yb and

Cp*₂Yb@SiO₂₋₇₀₀. D) EXAFS data (blue) and fits (red) in *k*-space (upper; top and right axes) and R-space (lower; bottom and left axes) of Cp*₂Yb@SiO₂₋₇₀₀.

Further information about the coordination environment of supported Yb centers is obtained by X-Ray Absorption Spectroscopy (XAS), performed at the Yb-L₁ edge. In the Yb L₁-edge XANES of Cp*₂Yb and Cp*₂Yb@SiO₂₋₇₀₀, nearly identical edge positions are observed, indicating that Yb remains in oxidation of +2 after grafting (Figure 1 C). Fitting the EXAFS data (Figure 1 D and Table S1) indicates the presence of five carbon atoms of the pentamethylcyclopentadienyl ring at 2.73(1) Å and five carbon atoms from the methyl carbons at 3.65(2) Å; Yb–O and Yb–Si distances are found at 2.24 Å and 3.21(3) Å, respectively. Additional scattering path from nearby siloxane bridges results in a similar statistical quality of the fit (see Table S2 and Figure S9) making it impossible to determine the presence of additional siloxane bridges interacting with the Yb centers from the EXAFS data (Scheme 2).

Cp*₂Sm and Cp*₂Sm@SiO₂₋₇₀₀ were also characterized by the Sm-L₁ edge. XANES spectra show that both have nearly identical edge positions indicating that the oxidation numbers of the two compounds are the same (Figure S10). It was not possible to obtain more information about the structure of the surface species due to the low intensity of the signals that precludes the accurate fitting of the EXAFS spectra (Figure S11). The ¹H MAS NMR spectrum of Cp*₂Sm@SiO₂₋₇₀₀ displays a single resonance at δ=1 ppm with a large anisotropy (Figure S7), typical for Sm^{II} species (vs. ca. 0 ppm in the case of Sm^{III} species). However, it was not possible to detect the ¹³C NMR resonances associated with the Sm^{II} surface species found at ca. δ(CH₃)= -98.2 ppm and δ(C_{ring})=99.0 ppm in solution.^{14f} Two resonances of weak intensity were observed at 11.2 and 113.8 ppm (Figure S8), suggesting the presence of small amount of Sm^{III} species,¹⁵ not detected by XAS, possibly formed during grafting either by reaction with surface hydroxyls, other sites or the released Cp*H.¹⁶

Cp*₂Yb@SiO₂₋₇₀₀ and Cp*₂Sm@SiO₂₋₇₀₀ polymerize ethylene at 50 °C and at 20 bar, in the absence of co-catalyst with an activity of 228 and 1280 kg_{PE} (mol_{Ln} h)⁻¹ respectively, which is ca. 3 and 4 times higher than for the parent molecular precursor, respectively (Table 1). The effect of grafting on the polymer

properties is striking with the production of ultrahigh molecular weight polyethylene (Table 1). Thus, the increased polymer chain length for the silica-supported metallocenes is associated with grafting, possibly because of site isolation and/or the exchange of one Cp* by a siloxy ligand. The CPMAS ^{13}C spectrum of the polymer produced by $\text{Cp}^*_2\text{Yb@SiO}_{2-700}$ does not show any end groups or any chain branching (Figure S6), consistent with the large M_n and M_w measured.

Table 1. Ethylene polymerization results.

	Activity ^[a]	M_n ^[b]	M_w ^[b]	\bar{D}
Cp^*_2Yb	74	100	350	3.6
$\text{Cp}^*_2\text{Yb@SiO}_{2-700}$	228	690	3570	5.2
Cp^*_2Sm	312	9	61	6.7
$\text{Cp}^*_2\text{Sm@SiO}_{2-700}$	1280	580	3210	5.6

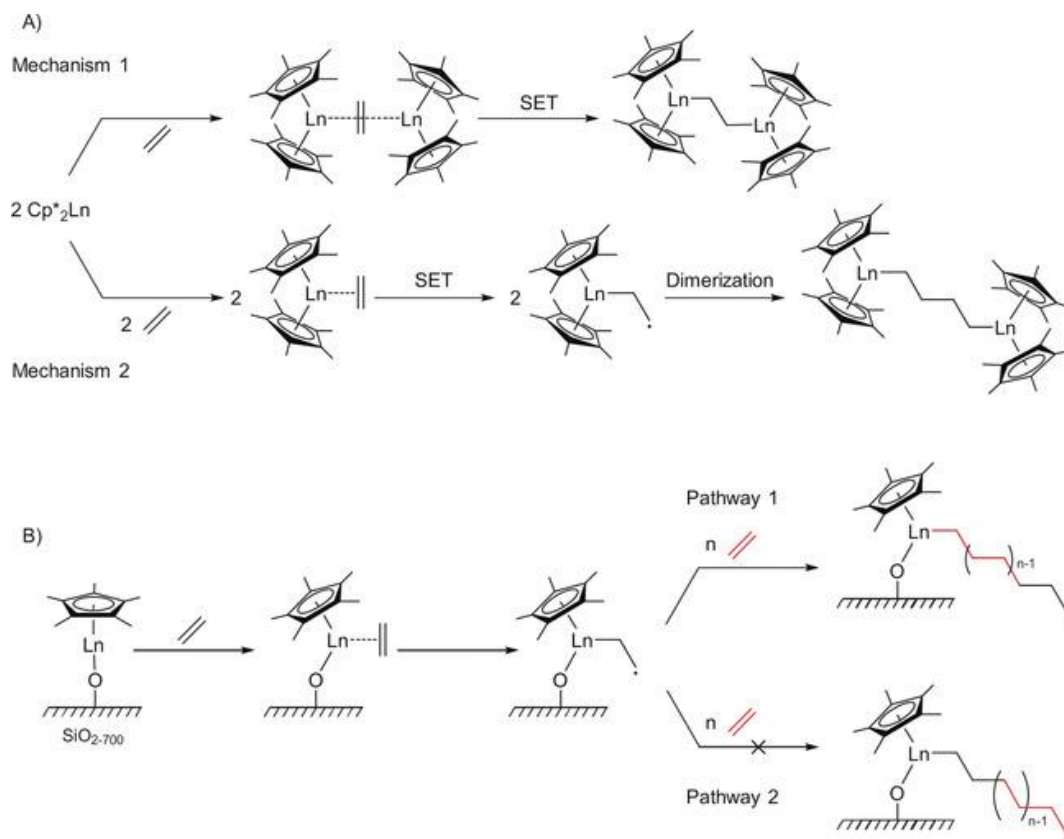
[a] Polymerization conditions: 50 °C, 20 bar. Unit: $\text{kg}_{\text{PE}} (\text{mol}_{\text{Ln}} \text{h})^{-1}$. [b] Determined by high-temperature size exclusion chromatography. Unit: kg mol^{-1} .

The number of active sites in $\text{Cp}^*_2\text{Yb@SiO}_{2-700}$ is determined by poisoning experiments using dimethoxyethane (Figure S13 A), since $\text{Cp}^*_2\text{Yb}(\text{OEt}_2)$ does not polymerize ethylene.^{11b} The polymerization activity of $\text{Cp}^*_2\text{Yb@SiO}_{2-700}$ decreases linearly with an increasing amount of poison reaching 0 when 0.25 equiv of dimethoxyethane per Yb is used, suggesting that only 25 % of the surface sites can initiate polymerization; this indicates that each active Yb center polymerizes with a rate close to $1000 \text{ kg}_{\text{PE}} (\text{mol}_{\text{Yb}} \text{h})^{-1}$. Since coordination of a single molecule of diethyl ether is sufficient to switch off its activity in the molecular system, it is possible that the coordination of nearby siloxane bridges leads to inactive species and accounts for the low number of active sites. Overall, the intrinsic activity of the active

centers is on average $1000 \text{ kg}_{\text{PE}} (\text{mol}_{\text{Yb}} \text{ h})^{-1}$, that is 12 times higher than that for the Cp^*_2Yb in solution. The supported Sm system also exhibits a linear decrease of activity with an increasing amount of dimethoxyethane but the number of active sites is only 10 % (Figure S13 B). This difference can be tentatively rationalized by the larger radius of the Sm^{2+} ion (136 pm vs. 116 pm for Yb^{2+}), favoring more interactions with neighboring siloxane bridge(s). Accordingly, the average activity of the active Sm sites is $12\,800 \text{ kg}_{\text{PE}} (\text{mol}_{\text{Sm}} \text{ h})^{-1}$, that is, 40 times higher than the parent Cp^*_2Sm .

In the case of the molecular complexes, Cp^*_2Yb and Cp^*_2Sm polymerize ethylene at 20°C , but Cp^*_2Eu is inactive. This is consistent with an initiation occurring through a single electron transfer (SET) process since Cp^*_2Yb and Cp^*_2Sm have redox potentials of -1.12 V and -1.7 V (vs. NHE) respectively, whereas that of Cp^*_2Eu is -0.56 V .¹⁷ Potential mechanisms involve the formation of a 2:1 complex of Cp^*_2Sm with ethylene, followed by SET¹⁸ (Scheme 3 A, Mechanism 1) or the formation of a 1:1 complex, followed by a SET and dimerization¹⁹ (Scheme 3 A, Mechanism 2). In order to assess whether or not the initiation also occurs through a SET in the case of the silica-supported lanthanocenes, we synthesize $\text{Cp}^*_2\text{Eu}@ \text{SiO}_{2-700}$ (see Figures S2 and S5 in the Supporting Information). The XAS at Eu-L₁ edge for Cp^*_2Eu and $\text{Cp}^*_2\text{Eu}@ \text{SiO}_{2-700}$ are nearly identical indicating Eu remains in a +2 oxidation state after grafting (Figure S12). The latter does not initiate polymerization, which supports the SET process postulated for Ln=Yb and Sm. Initiation through a SET process is consistent with the inactivity of $\text{Cp}^*_2\text{Ln}@ \text{SiO}_{2-700}$ (Ln=Yb and Sm) towards propylene polymerization, since in gas phase the propylene anion is 0.21 eV ($4.9 \text{ kcal mol}^{-1}$) higher in energy than the ethylene anion.²⁰ Furthermore, grafting onto SiO_{2-700} imposes site isolation (<1 Ln center per square nanometer), ruling out the formation of a 2:1 complex (Scheme 3 A, Mechanism 1) and/or preventing the putative Ln alkyl radical to dimerize on the surface (Scheme 3 A, Mechanism 2). The linear decrease of the activity with increasing amount of poison indicates a monometallic initiation, forming $[(\equiv\text{SiO})(\text{Cp}^*)\text{Ln}^{3+}(-\text{CH}_2-\text{CH}_2\cdot)]$ that initiates chain growth either by coordination of ethylene followed by insertion into the Ln–C bond (Scheme 3 B, Pathway 1) or through radical propagation (Scheme 3 B, Pathway 2). Since the activity depends strongly on the lanthanide metal, $\text{Sm} > \text{Yb}$, chain growth most likely takes place through the Cossee–Arlman mechanism,

as shown with Cp^*_2LuMe ²¹ and suggested for Cp^*_2YbMe .²² This pathway generates a long chain polymer with a long-lived carbon-based free radical that can be observed by EPR spectroscopy.²³



Scheme 3. A) Initiation of ethylene polymerization of Cp^*_2Ln . B) Initiation of ethylene polymerization of $\text{Cp}^*_2\text{Ln}@ \text{SiO}_2\text{-700}$ and further chain growth.

In summary, we have described the formation and characterization of highly reactive heterogeneous catalysts for ethylene polymerization through grafting of Cp^*_2Ln on silica via SOMC. Similar to some industrial catalysts such as the Philipps and Union Carbide systems, both $\text{Cp}^*_2\text{Yb}@ \text{SiO}_2\text{-700}$ and $\text{Cp}^*_2\text{Sm}@ \text{SiO}_2\text{-700}$ have no metal-alkyl group present initially, yet these supported species initiate ethylene polymerization in the absence of co-catalysts. Despite the low number of active sites, their intrinsic activity is strikingly high, 1000 and 12 800 $\text{kg}_{\text{PE}} (\text{mol}_{\text{Ln}} \text{h})^{-1}$ for Yb and Sm, respectively, exceeding those of the parent molecular precursors, further illustrating the advantage of site isolation. Initiation takes place through a single electron transfer to generate the active surface species $[(\equiv\text{SiO})\text{Ln}^{3+}(\text{Cp}^*)(-\text{CH}_2\text{---CH}_2)]$.

The specificity of these Yb/Sm supported catalysts for ethylene over propylene is also observed in the Phillips and the Union Carbide (silica-supported chromocene) catalysts. The reactivity pattern of these metallocene catalysts triggers the thought that they share a common initiation mechanism, a connection that is under active study in our laboratories.

Acknowledgements

F.A. was supported by a Marie Curie fellowship (FP7-PEOPLE-2012-ITN number 317127) and K.-W.C. by SNF (200021L_157146). A.F. thanks the Holcim Stiftung for a habilitation fellowship. We acknowledge PSI for beamtime. We thank Dr. Olga V. Safonova and Dr. Victor Mougel for assistance with EXAFS measurements and fruitful discussions, respectively. Dr. Romain Berthoud and Dr. John Severn are acknowledged for HT-SEC measurements.

References

- [1] a) A. Valente, A. Mortreux, M. Visseaux, P. Zinck, *Chem. Rev.* 2013, 113, 3836–3857; b) S. B. Amin, T. J. Marks, *Angew. Chem. Int. Ed.* 2008, 47, 2006–2025; *Angew. Chem.* 2008, 120, 2034 – 2054.
- [2] a) E. Y.-X. Chen, T. J. Marks, *Chem. Rev.* 2000, 100, 1391–1434; b) M. Bochmann, *Organometallics* 2010, 29, 4711–4740; c) M. C. Baier, M. A. Zuideveld, S. Mecking, *Angew. Chem. Int. Ed.* 2014, 53, 9722–9744; *Angew. Chem.* 2014, 126, 9878 – 9902.
- [3] W. Kaminsky, *J. Chem. Soc. Dalton Trans.* 1998, 1413–1418.
- [4] a) J. Joubert, F. Delbecq, P. Sautet, E. L. Roux, M. Taoufik, C. Thieuleux, F. Blanc, C. Cop8ret, J. Thivolle-Cazat, J.-M. Basset, *J. Am. Chem. Soc.* 2006, 128, 9157–9169; b) M. Jezequel, V. Dufaud, M. J. Ruiz-Garcia, F. Carrillo-Hermosilla, U. Neugebauer, G. P. Niccolai, F. Lefebvre, F. Bayard, J. Corker, S. Fiddy, J. Evans, J.-P. Broyer, J. Malinge, J.-M. Basset, *J. Am. Chem. Soc.* 2001, 123, 3520–

3540; c) M. Y. He, G. Xiong, P. J. Toscano, R. L. Burwell, Jr., T. J. Marks, *J. Am. Chem. Soc.* 1985, 107, 641–652.

[5] a) H. Ahn, T. J. Marks, *J. Am. Chem. Soc.* 1998, 120, 13533 – 13534; b) H. Ahn, C. P. Nicholas, T. J. Marks, *Organometallics* 2002, 21, 1788–1806; c) L. A. Williams, T. J. Marks, *Organometallics* 2009, 28, 2053–2061; d) L. A. Williams, T. J. Marks, *ACS Catal.* 2011, 1, 238–245; e) L. A. Williams, N. Guo, A. Motta, M. Delferro, I. L. Fragal/, J. T. Miller, T. J. Marks, *Proc. Natl. Acad. Sci. USA* 2013, 110, 413–418; f) W. Gu, M. M. Stalzer, C. P. Nicholas, A. Bhattacharyya, A. Motta, J. R. Gallagher, G. Zhang, J. T. Miller, T. Kobayashi, M. Pruski, *J. Am. Chem. Soc.* 2015, 137, 6770–6780.

[6] J. R. Severn, J. C. Chadwick, R. Duchateau, N. Friederichs, *Chem. Rev.* 2005, 105, 4073–4147.

[7] M. P. McDaniel, *Adv. Catal.* 2010, 53, 123–606.

[8] a) M. P. Conley, M. F. Delley, G. Siddiqi, G. Lapadula, S. Norsic, V. Monteil, O. V. Safonova, C. Cop8ret, *Angew. Chem. Int. Ed.* 2014, 53, 1872–1876; *Angew. Chem.* 2014, 126, 1903–1907; b) M. F. Delley, F. NfflÇez-Zarur, M. P. Conley, A. Comas-Vives, G. Siddiqi, S. Norsic, V. Monteil, O. V. Safonova, C. Cop8ret, *Proc. Natl. Acad. Sci. USA* 2014, 111, 11624–11629; c) M. F. Delley, G. Lapadula, F. NfflÇez-Zarur, A. Comas-Vives, V. Kalendra, G. Jeschke, D. Baabe, M. D. Walter, A. J. Rossini, A. Lesage, L. Emsley, O. Maury, C. Cop8ret, *J. Am. Chem. Soc.* 2017, 139, 8855–8867.

[9] H. Ikeda, T. Monoi, Y. Sasaki, *J. Polym. Sci. Part A* 2003, 41, 413–419.

[10] a) F. J. Karol, G. L. Karapinka, C. Wu, A. W. Dow, R. N. Johnson, W. L. Carrick, *J. Polym. Sci., Part A-1* 1972, 10, 2621–2637; b) G. Karapinka, Google Patents, 1973; c) M. Schnellbach, F. Kçhler, J. Blgmel, *J. Organomet. Chem.* 1996, 520, 227–230; d) K. H. Theopold, *Eur. J. Inorg. Chem.* 1998, 15–24.

[11] a) T. D. Tilley, R. A. Andersen, B. Spencer, H. Ruben, A. Zalkin, D. H. Templeton, *Inorg. Chem.* 1980, 19, 2999–3003; b) C. E. Kefalidis, L. Perrin, C. J. Burns, D. J. Berg, L. Maron, R. A. Andersen,

- Dalton Trans. 2015, 44, 2575–2587; c) Z. Hou, Y. Wakatsuki, *Coord. Chem. Rev.* 2002, 231, 1–22; d) Z. Hou, Y. Zhang, H. Tezuka, P. Xie, O. Tardif, T.-a. Koizumi, H. Yamazaki, Y. Wakatsuki, *J. Am. Chem. Soc.* 2000, 122, 10533–10543; e) F. T. Edelman, in *Organolanthoid Chemistry: Synthesis Structure, Catalysis*, Springer, Berlin, 1996, pp. 247–276; f) W. J. Evans, L. A. Hughes, T. P. Hanusa, *J. Am. Chem. Soc.* 1984, 106, 4270–4272; g) M. Schultz, C. J. Burns, D. J. Schwartz, R. A. Andersen, *Organometallics* 2000, 19, 781–789. [12] a) C. Cop8ret, A. Comas-Vives, M. P. Conley, D. P. Estes, A. Fedorov, V. Mougel, H. Nagae, F. NfflÇez-Zarur, P. A. Zhizhko, *Chem. Rev.* 2016, 116, 323–421; b) C. Cop8ret, F. Allouche, K. W. Chan, M. P. Conley, M. F. Delley, A. Fedorov, I. B. Moroz, V. Mougel, M. Pucino, K. Searles, K. Yamamoto, P. A. Zhizhko, *Angew. Chem. Int. Ed.* 2018, DOI: 10.1002/ange.201702387.
- [13] P. Selg, H. H. Brintzinger, M. Schultz, R. A. Andersen, *Organometallics* 2002, 21, 3100–3107.
- [14] L. Maron, L. Perrin, O. Eisenstein, R. Andersen, *J. Am. Chem. Soc.* 2002, 124, 5614–5615.
- [15] W. J. Evans, J. W. Grate, I. Bloom, W. E. Hunter, J. L. Atwood, *J. Am. Chem. Soc.* 1985, 107, 405–409.
- [16] W. J. Evans, T. A. Ulibarri, *J. Am. Chem. Soc.* 1987, 109, 4292 – 4297.
- [17] R. Finke, S. Keenan, D. Schiraldi, P. Watson, *Organometallics* 1986, 5, 598–601.
- [18] a) W. J. Evans, D. M. DeCoster, J. Greaves, *Macromolecules* 1995, 28, 7929–7936; b) W. J. Evans, T. A. Ulibarri, J. W. Ziller, *J. Am. Chem. Soc.* 1988, 110, 6877–6879; c) W. J. Evans, D. K. Drummond, S. G. Bott, J. L. Atwood, *Organometallics* 1986, 5, 2389–2391; d) W. J. Evans, T. A. Ulibarri, J. W. Ziller, *J. Am. Chem. Soc.* 1990, 112, 219–223; e) W. J. Evans, R. A. Keyer, J. W. Ziller, *Organometallics* 1993, 12, 2618–2633.
- [19] L. S. Boffa, B. M. Novak, *Tetrahedron* 1997, 53, 15367–15396.
- [20] a) K. D. Jordon, J. A. Michejda, P. D. Borrow, *Chem. Phys. Lett.* 1976, 42, 227; b) K. D. Jordon, P. D. Borrow, *Chem. Rev.* 1987, 87, 557.

[21] a) P. L. Watson, *J. Am. Chem. Soc.* 1982, 104, 337–339; b) P. L. Watson, T. Herskovitz, *ACS Symposium Series*, 1983, 212, 458—479.

[22] M. D. Walter, P. T. Matsunaga, C. J. Burns, L. Maron, R. A. Andersen, *Organometallics* 2017, 36, 4564–4578.

[23] P. O'Neill, C. Birkinshaw, J. J. Leahy, R. Barklie, *Polym. Degrad. Stab.* 1999, 63, 31–39.